ChemComm

Chemical Communications

Accepted Manuscript

Volume 54
Number 1
4 January 2018
Pages 1-112

ChemComm

Chemical Communications

rsc.li/chemcomm

ISSN 1359-7345

COMMUNICATION
S. J. Connon, M. O. Senge et al
Conformational control of nonplanar free base porphyrins:
towards bifunctional catalysts of tunable basicity

ROYAL SOCIETY
OF CHEMISTRY

ROYAL SOCIETY
OF CHEMISTRY

rsc.li/chemcomm

COMMUNICATION

Development of a near-infrared fluorescence probe for hypochlorous acid based on the phenyl-induced twisted intramolecular charge transfer (p-TICT) mechanism

Hisashi Ohno,[a] Shun Sumitani,[a] Ariunbold Chuluun-Erdene,[b] Takahiro Kuchimaru,[b] Sota Yamada,[a,c] Eita Sasaki,[a,c] and Kenjiro Hanaoka[a,c,*]

Near-infrared (NIR) fluorescence probes for hypochlorous acid (HClO) are powerful tools for investigating various biological phenomena because of their low autofluorescence, high tissue penetration and usefulness for multicolour imaging. Here we present a rational probe design strategy based on the phenyl-induced twisted intramolecular charge transfer (p-TICT) mechanism and apply it to develop a NIR fluorescence probe for HClO, *N*-Phenol SiR1. This probe was applied for live-cell fluorescence imaging multicolor (4 colors), occupying the NIR color window.

Highly reactive oxygen species (hROS) are involved in biological redox systems and mediate a variety of biological phenomena.[1] Hypochlorous acid (HClO) is one of the hROS and is produced mainly in leukocytes, including neutrophils, macrophages and monocytes, through the myeloperoxidase (MPO)-catalyzed peroxidation of chloride ions with H_2O_2. It is deeply related to host defense, playing a vital role in killing a wide range of pathogens.[2] It is also considered that neutrophil-derived HClO contributes to inflammation-associated tissue injury, such as hepatic ischemia-reperfusion injury,[3] atherosclerosis,[4] lung injury[5] and rheumatoid arthritis.[6] So far, many fluorescence probes have been developed for HClO detection.[7,8] On the other hand, several fluorescence probes emitting NIR fluorescence have been developed in recent years, especially for the far-red to NIR color window in multicolour imaging and for whole-body imaging. However, fluorescence probes based on photoinduced electron transfer (PET) show a relatively small fluorescence increase upon reaction with HClO.[9] Intramolecular spirocyclization-based probes exhibit a large fluorescence increase, but the complete lack of fluorescence before the reaction with HClO can make it difficult to judge whether or not the fluorescence probe has been loaded into the cells.[10]

Therefore, to overcome these issues, we set out to develop a NIR fluorescence probe for HClO based on a different fluorescence off/on mechanism, which would exhibit weak fluorescence before the reaction with HClO, but generate a large fluorescence increase upon reaction with HClO.

Recently, we have reported that a large fluorescence off/on change of rhodamines having a phenyl group on the N atom of the xanthene ring can be achieved by utilizing the phenyl-induced twisted intramolecular charge transfer (p-TICT) mechanism (Fig. 1a).[11] The introduction of a phenyl group on the N atom of the xanthene ring induces a structural change to a twisted intramolecular charge transfer (TICT) excited state upon photoirradiation, and non-radiative relaxation from the excited state results in no fluorescence. In this work, we utilized
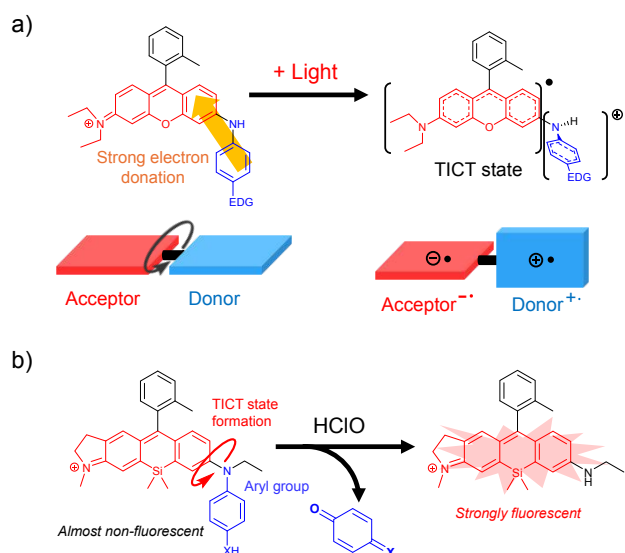

Fig 1. (a) Schematic illustration of the photoirradiation-induced TICT state formation of rhodamine having an aryl group with an electron-donating group (EDG) at the N atom of the xanthene ring.[11] The acceptor or donor moiety is shown in red or blue, respectively. (b) Design of a fluorescence probe for HClO based on the p-TICT mechanism. X = OH or NH_2.

[a] Graduate School of Pharmaceutical Sciences, Keio University, Tokyo 105-8512, Japan. E-mail: khanaoka@keio.jp
[b] Division of Bioconvergence, Center for Molecular Medicine, Jichi Medical University, Tochigi 329-0498, Japan.
[c] Faculty of Pharmacy, Keio University, Tokyo 105-8512, Japan.

Electronic Supplementary Information (ESI) available: [details of any supplementary information available should be included here]. See DOI: 10.1039/x0xx00000x

COMMUNICATION

the p-TICT mechanism to design a novel NIR fluorescence probe for HClO (Fig. 1b). In the molecular design, we employed the Si-rhodamine scaffold, which emits NIR fluorescence,[12] and we introduced a phenol or an aniline moiety into the rhodamine scaffold as the HClO-reactive moiety. The phenol or aniline moiety is expected to be oxidised by HClO and released as a quinone, causing the probe to become strongly fluorescent.[13]

Our group has previously synthesized a wide variety of unsymmetrical Si-rhodamines by means of heterodimerization reaction between a *p*-hydroxymethyl aniline and an aniline as the key reaction.[12] Moreover, we newly established methodology to introduce an electron-rich aromatic ring into the amino group of the xanthone ring of the rhodamines by means of Buchwald-Hartwig cross-coupling (Scheme S1). Using these methods, we synthesized two probe candidates, **N-Phenol SiR1** which has a phenol moiety as the reaction moiety for HClO and **N-Aniline SiR** which has an aniline moiety as the reaction moiety, as well as a control probe, **N-Ph SiR** (Fig. 2a). We also synthesized the product, **N-Et SiR**, expected to be formed by the reaction of **N-Phenol SiR1** or **N-Aniline SiR** with HClO. We then examined the photophysical properties of these compounds. They exhibited almost the same absorption spectra and molar extinction coefficients (ε) (Fig. 2b and Table S1) and showed high photostability (Fig. S1).[14] **N-Phenol SiR1**, **N-Aniline SiR** and **N-Ph SiR** exhibited very weak fluorescence ($\Phi_{fl} < 0.01$), while **N-Et SiR** showed strong fluorescence (Fig. 2b and Table 1).

To verify the fluorescence quenching mechanism, the viscosity-dependence of the fluorescence intensity of **N-Ph SiR**, **N-Phenol SiR1** or **N-Aniline SiR** was examined (Fig. S2). We previously reported that the p-TICT process in these rhodamines having a phenyl group at the N atom of the xanthene ring is partially inhibited under high viscosity conditions, where the rotation of the Ph group is restricted.[11] We measured the fluorescence spectra of **N-Ph SiR**, **N-Phenol SiR1** and **N-Aniline SiR** in PBS, ethanol, ethylene glycol and glycerol. All the probes showed absorbance at around 670 nm in all solvents (Fig S3), On the other hand, **N-Ph SiR** and **N-Phenol SiR1** showed a fluorescence increase that was dependent on the solvent viscosity, while **N-Aniline SiR** showed only a slight increase in fluorescence even in glycerol, probably due to the strong electron-donating ability of the aniline moiety. We performed TD-DFT calculations to further investigate the influence of the electron-donating group introduced at the *para*-position of the phenyl group on the TICT process. The relationship between the C_{aryl}–N bond rotation and the total energy of **N-Ph SiR**, **N-Phenol SiR1** and **N-Aniline SiR** in the ground and excited states was calculated at the CAM-B3LYP 6-31G+(d,p) level (Fig. S4 and S5). The probes all showed a total energy minimum around dihedral angle $\phi = 90°$ in the excited state, demonstrating the presence of the TICT state (Fig. S4d-f), and their oscillator strengths of the $S_1 \rightarrow S_0$ transition around 90° were less than 0.1, in accordance with the previous study.[11] **N-Aniline SiR** also showed greater stabilization in terms of the total energy of its TICT excited state ($\phi = 90°$) compared with the other probes, probably because of the stronger electron-donating ability of the amino group than -OH and -H.

These results are consistent with fluorescence quenching through the p-TICT process in all the probes.
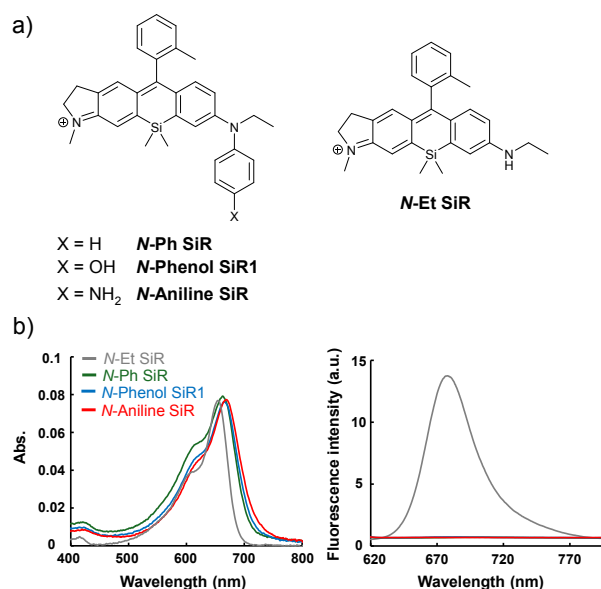

Fig. 2 (a) The structures of synthesized probes, including the control probe (**N-Ph SiR**) and the expected product after the reaction of **N-Phenol SiR1** or **N-Aniline SiR** with HClO (**N-Et SiR**). (b) Absorption (left) and fluorescence (right) spectra of **N-Phenol SiR1**, **N-Aniline SiR**, **N-Ph SiR** and **N-Et SiR**. The excitation wavelength was 600 nm. The slit widths for excitation and emission were both 5 nm.

Next, we examined the reactivities of **N-Phenol SiR1** and **N-Aniline SiR** with various ROS (reactive oxygen species) based on the fluorescence increase after the reaction. **N-Phenol SiR1** and **N-Aniline SiR** showed a rapid and large fluorescence increase from $\Phi_{fl} < 0.01$ to $\Phi_{fl} = 0.14$ and 0.18, respectively, upon reaction with 5 μM HClO (Fig. 3a,b). Although these probes also showed a fluorescence increase upon reaction with ONOO⁻, their reactivity with ONOO⁻ was lower than that with HClO (Fig. 3c,d). On the other hand, they exhibited almost no fluorescence increase even after 30 min upon reaction with other reactive oxygen species ($O_2^{-\bullet}$, H_2O_2, $^\bullet NO$, $^1O_2$, TBHP and $^\bullet OH$).

To examine the importance of the Me group in the upper benzene moiety of **N-Phenol SiR1**, we also synthesized **N-Phenol SiR2**, which is a **N-Phenol SiR1** analogue having a carboxy group instead of the Me group (Fig. S6, S7). **N-Phenol SiR2** showed a relatively low ε, probably because there is a spirocyclization equilibrium between the open (fluorescent) and closed (nonfluorescent) forms.[15] Moreover, **N-Phenol SiR2** showed no fluorescence change upon reaction with HClO or ONOO⁻ (Fig. S8a). We consider that the change in the electron density of the reaction moiety of the probe, i.e., the phenol moiety, upon intramolecular spirocyclization is likely to be the predominant contributor to this low reactivity with HClO and ONOO⁻. We further examined the importance of the indoline substructure of the xanthene ring. We designed and synthesized **N-Phenol SiR3**, which is a **N-Phenol SiR1** analogue having the tetrahydroquinoline structure instead of the indoline

structure (Fig. S6). **N-Phenol SiR3** showed almost the same photophysical properties as **N-Phenol SiR1** and its fluorescence was also strongly quenched. The reactivity of **N-Phenol SiR3** with various ROS was almost the same as that of **N-Phenol SiR1** (Fig. S8b). We then analyzed the reaction products of **N-Phenol SiR1** and **N-Aniline SiR** upon reaction with HClO and ONOO⁻ by HPLC (Fig. S9, S10). The peak corresponding to **N-Et SiR** was detected as a major product after the reaction of each probe with HClO or ONOO⁻; thus, the reaction of each probe with HClO proceeded with release of the reaction moiety as shown in Fig. 1b.
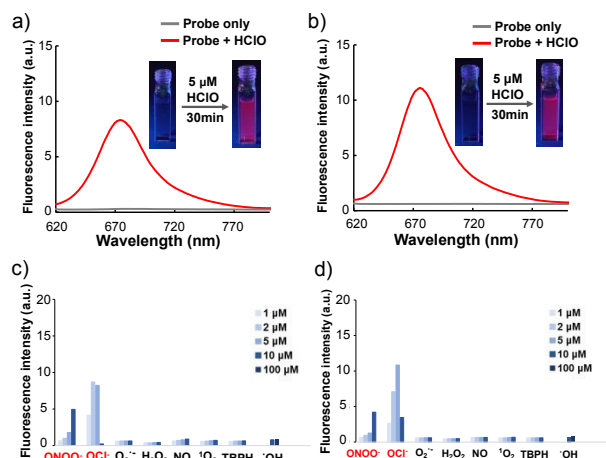

Fig. 3 (a,b) Fluorescence spectra of 1 μM (a) **N-Phenol SiR1** and (b) **N-Aniline SiR** before (grey line) and after (red line) reaction with 5 μM HClO for 30 min. The excitation wavelength was 600 nm. (c,d) Fluorescence intensities at 672 nm of 1 μM (c) **N-Phenol SiR1** and (d) **N-Aniline SiR** after reaction with various ROS. The fluorescence measurements were performed in PBS with excitation at 600 nm at 37°C for 30 min. The slit widths for excitation and emission were both 5 nm. ONOO⁻: ONOONa; ⁻OCl: NaOCl; $O_2^{\bullet-}$: KO₂; H₂O₂; NO: NOC 7 (0.5 eq.); ¹O₂: EP-1; TBHP: t-BuOOH; •OH: 100 mM (or 1 M) H₂O₂ and 10 μM (or 100 μM) FeCl₂ (Fenton reaction).

We then examined the reactivities of **N-Phenol SiR1** and **N-Aniline SiR** with HClO, which was generated from MPO, by measuring the fluorescence intensity changes over time (Fig. S11). After addition of H₂O₂ to the probe solution, HClO was generated via the enzymatic activity of MPO. Both probes showed a large fluorescence increase after addition of H₂O₂, and this fluorescence increase was suppressed upon addition of the MPO inhibitor 4-aminobenzohydrazide (4-ABHA). Thus, both probes react with HClO generated by MPO from Cl⁻ with H₂O₂, resulting in a fluorescence increase.

We then applied **N-Phenol SiR1** and **N-Aniline SiR** to the live-cell fluorescence imaging of HClO in HL60 cells (Fig. 4). HL60 cells, which express MPO, were incubated with **N-Phenol SiR1** or **N-Aniline SiR** followed by the addition of H₂O₂ for the generation of HClO by MPO, as shown in Fig. 4b. We observed a fluorescence increase in living cells incubated with **N-Phenol SiR1** within 10 min after addition of H₂O₂ and this fluorescence increase was significantly suppressed by the MPO inhibitor 4-

ABHA (Fig. 4c). On the other hand, **N-Aniline SiR** showed very weak fluorescence before H₂O₂ addition compared with **N-Phenol SiR1** (Fig. 4a,d) and this is consistent with low cell-membrane permeability of **N-Aniline SiR**. To investigate this difference, we examined the subcellular localization of each probe (Fig S12). **N-Phenol SiR1** was mainly localized in the mitochondria and partly in lysosomes, while **N-Aniline SiR** was mainly localized in lysosomes. We then examined the reactivity of each probe with HClO at various pH values, because lysosomes are acidic organelles. It was found that both probes showed comparable fluorescence increases upon reaction with HClO between pH 4-9 (Fig. S13). Based on these results, we concluded that **N-Aniline SiR** could not efficiently penetrate the cell membrane due to its high water solubility. Thus, **N-Phenol SiR1** could detect HClO in cells containing ROS scavengers such as biothiols and metal ions.[16]
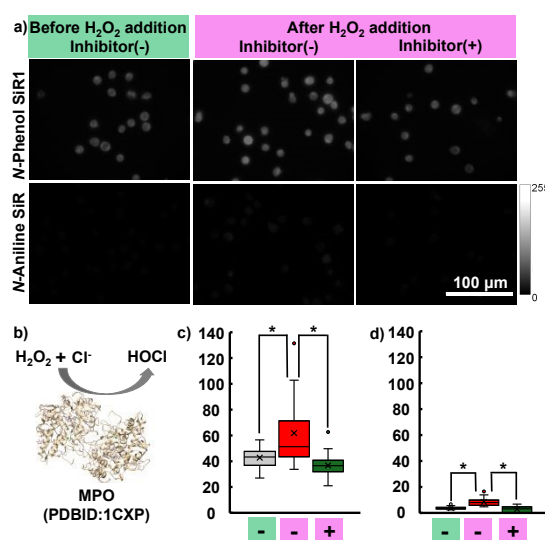

Fig. 4 Application of **N-Phenol SiR1** and **N-Aniline SiR** for live-cell fluorescence imaging. (a) Fluorescence microscopic images of HL 60 cells incubated with 1 μM **N-Phenol SiR1** or **N-Aniline SiR** for 15 min, with or without the MPO inhibitor (4-ABHA), before and after addition of H₂O₂. (b) The MPO-based generation system of HClO from H₂O₂ and chloride ion. (c) Fluorescence intensities of HL60 cells incubated with **N-Phenol SiR1**, from the fluorescence images of (a). (d) Fluorescence intensities of HL60 cells incubated with **N-Aniline SiR**, from the fluorescence images of (a). Error bars represent ± S.E. (n = 25). * Indicates p < 0.01 (Welch's t-test).

We next applied **N-Phenol SiR1** for imaging endogenous HClO of murine neutrophils (Fig. S14). Murine neutrophils, isolated from C57BL/6 mice, were incubated with **N-Phenol SiR1** followed by stimulation with phorbol 12-myristate 13-acetate (PMA) to generate HClO in phagosomes, in which the pH is acidic.[17] After the PMA stimulation, **N-Phenol SiR1** showed a large fluorescence increase, which was significantly suppressed in the presence of 4-ABAH. These results indicate that the **N-Phenol SiR1** could detect endogenously generated HClO in neutrophils. We further examined multicolour imaging of phagocytosis by murine neutrophils, using **N-Phenol SiR1** as

COMMUNICATION

a far-red to near-infrared (NIR) window (Fig. 5). When *E. coli* expressing sfGFP (*E. coli*/sfGFP) as a green window was labelled with both **N-Phenol SiR1** and pHrodoRed (a red fluorescence probe for detecting acidic pH) was added to murine neutrophils stained with CellTraceViolet (a blue fluorescent cell tracker dye), we observed that the neutrophils engulfed *E. coli* with enhancement of the fluorescence signals of **N-Phenol SiR1** and pHrodoRed. These results indicate that **N-Phenol SiR1** can be used for multicolor imaging as a fluorescence probe for HClO detection functioning in the NIR color window.
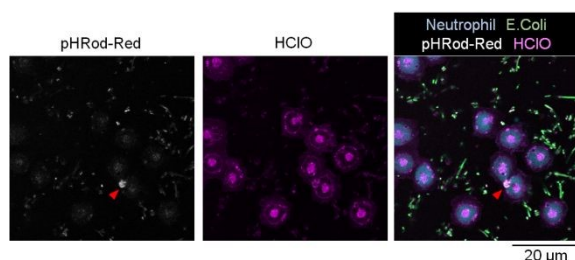

Fig. 5 Multicolor imaging of the phagocytosis of *E. coli* expressing sfGFP (*E. coli*/sfGFP) labelled with **N-Phenol SiR1** and pHrodoRed by murine neutrophils (right). HClO generation (middle) and pH decrease (left) in the phagosome were detected with **N-Phenol SiR1** (far-red to NIR window: ex. 638 nm, em. 660-700 nm) and pHrodoRed (red window: ex. 552 nm, em. 570-630 nm), respectively. The presence of *E. coli* was monitored with GFP (green window: ex. 488 nm, em. 505-550 nm) and neutrophils were labelled with the blue cell tracker (CellTraceViolet; blue window: ex. 405 nm, em. 420-480 nm). The red arrowheads in the images indicate phagosome formation with a strong fluorescence signal of pHrodo Red.

In conclusion, we have rationally designed and successfully developed **N-Phenol SiR1** as an Si-rhodamine-based NIR fluorescence probe for HClO, utilizing the p-TICT mechanism. The developed probe could visualize HClO endogenously generated in neutrophils in the far-red to NIR region, demonstrating its usefulness for multicolor imaging. Although a few hROS probes based on the p-TICT mechanism had been reported even before we elucidated the detailed mechanism of the p-TICT system,[18,19] they operate in the visible region and detect hROS species other than HClO. Our present results confirm that the p-TICT mechanism is a useful fluorescence control principle for developing fluorescence probes. We expect that our developed fluorescence probe for HClO will be a useful tool in studies of redox biology for multicolor imaging.

Data availability

The data supporting this article have been included as part of the ESI. The datasets in the current study are available from the corresponding author upon reasonable request.

Conflicts of interest

There are no conflicts to declare.

Notes and references

1 J. D. Lambeth, *Free Radic. Biol. Med.*, 2007, **43**, 332–347.
2 A. J. Kettle and C. C. Winterbourn, *Redox Rep.*, 1997, **3**, 3–15.
3 T. Hasegawa, E. Malle, A. Farhood and H. Jaeschke, *Am. J. Physiol. Gastrointest. Liver Physiol.*, 2005, **289**, G760-7.
4 A. Daugherty, J. L. Dunn, D. L. Rateri and J. W. Heinecke, *J. Clin. Invest.*, 1994, **94**, 437–444.
5 S. Hammerschmidt, N. Büchler and H. Wahn, *Chest*, 2002, **121**, 573–581.
6 S. M. Wu and S. V. Pizzo, *Arch. Biochem. Biophys.*, 2001, **391**, 119–126.
7 S. Kenmoku, Y. Urano, H. Kojima and T. Nagano, *J. Am. Chem. Soc.*, 2007, **129**, 7313–7318.
8 Y. Yue, F. Huo, C. Yin, J. O. Escobedo and R. M. Strongin, *Analyst*, 2016, **141**, 1859–1873.
9 Y. Koide, M. Kawaguchi, Y. Urano, K. Hanaoka, T. Komatsu, M. Abo, T. Terai and T. Nagano, *Chem. Commun.*, 2012, **48**, 3091–3093.
10 Y. Koide, Y. Urano, K. Hanaoka, T. Terai and T. Nagano, *J. Am. Chem. Soc.*, 2011, **133**, 5680–5682.
11 K. Hanaoka, S. Iwaki, K. Yagi, T. Myochin, T. Ikeno, H. Ohno, E. Sasaki, T. Komatsu, T. Ueno, M. Uchigashima, T. Mikuni, K. Tainaka, S. Tahara, S. Takeuchi, T. Tahara, M. Uchiyama, T. Nagano and Y. Urano, *J. Am. Chem. Soc.*, 2022, **144**, 19778–19790.
12 K. Hanaoka, Y. Kagami, W. Piao, T. Myochin, K. Numasawa, Y. Kuriki, T. Ikeno, T. Ueno, T. Komatsu, T. Terai, T. Nagano and Y. Urano, *Chem. Commun.*, 2018, **54**, 6939–6942.
13 K.-I. Setsukinai, Y. Urano, K. Kakinuma, H. J. Majima and T. Nagano, *J. Biol. Chem.*, 2003, **278**, 3170–3175.
14 Y. Koide, Y. Urano, K. Hanaoka, W. Piao, M. Kusakabe, N. Saito, T. Terai, T. Okabe and T. Nagano, *J. Am. Chem. Soc.*, 2012, **134**, 5029–5031.
15 G. Lukinavičius, K. Umezawa, N. Olivier, A. Honigmann, G. Yang, T. Plass, V. Mueller, L. Reymond, I. R. Corrêa Jr, Z.-G. Luo, C. Schultz, E. A. Lemke, P. Heppenstall, C. Eggeling, S. Manley and K. Johnsson, *Nat. Chem.*, 2013, **5**, 132–139.
16 G. Gille and K. Singer, *Folia Microbiol.*, 1995, **40**, 131-152.
17 L. Nault, L. Bouchab, S. Dupré-Crochet, O. Nüße and M. Erard, *Antioxid. Redox Signal.*, 2016, **25**, 564–576.
18 T. Peng, N.-K. Wong, X. Chen, Y.-K. Chan, Z. Sun, J. J. Hu, J. Shen, H. El-Nezami and D. Yang, *J. Am. Chem. Soc.*, 2014, **136**, 11728–11734.
19 T. Peng, X. Chen, L. Gao, T. Zhang, W. Wang, J. Shen and D. Yang, *Chem. Sci.*, 2016, **7**, 5407–5413.

The data supporting this article have been included as part of the ESI. The datasets in the current study are available from the corresponding author upon reasonable request.

ChemComm Accepted Manuscript